

# Evidence for a Population Expansion in the West Nile Virus Vector *Culex tarsalis*

Meera Venkatesan,\* Catherine J. Westbrook,† M. Claire Hauer,\*‡ and Jason L. Rasgon\*‡

\*The W. Harry Feinstone Department of Molecular Microbiology and Immunology, Bloomberg School of Public Health, Johns Hopkins University; †Florida Medical Entomology Laboratory, University of Florida; and ‡The Johns Hopkins Malaria Research Institute, Bloomberg School of Public Health, Johns Hopkins University

Population genetic structure of the West Nile Virus vector *Culex tarsalis* was investigated in 5 states in the western United States using 5 microsatellite loci and a fragment of the mitochondrial reduced form of nicotinamide adenine dinucleotide dehydrogenase 4 (ND4) gene. ND4 sequence analysis revealed a lack of isolation by distance, panmixia across all populations, an excess of rare haplotypes, and a star-like phylogeny. Microsatellites revealed moderate genetic differentiation and isolation by distance, with the largest genetic distance occurring between populations in southern California and New Mexico ( $F_{ST} = 0.146$ ). Clustering analysis and analysis of molecular variance on microsatellite data indicated the presence of 3 broad population clusters. Mismatch distributions and site-frequency spectra derived from mitochondrial ND4 sequences displayed pattern's characteristic of population expansion. Fu and Li's  $D^*$  and  $F^*$ , Fu's  $F_S$ , and Tajima's  $D$  statistics performed on ND4 sequences all revealed significant, negative deviations from mutation-drift equilibrium. Microsatellite-based multilocus heterozygosity tests showed evidence of range expansion in the majority of populations. Our results suggest that *C. tarsalis* underwent a range expansion across the western United States within the last 375,000–560,000 years, which may have been associated with Pleistocene glaciation events that occurred in the midwestern and western United States between 350,000 and 1 MYA.

## Introduction

*Culex tarsalis* is implicated as a major mosquito vector of West Nile Virus (WNV) in the western United States (Goddard et al. 2002, Reisen et al. 2004, Bell et al. 2005, Turell et al. 2005, DiMenna et al. 2006). The geographic range of *C. tarsalis* spans from the west coast to the Mississippi River and from northern Mexico to Canada (Darsie and Ward 1981). Larvae can develop in various freshwater habitats (Reisen and Reeves 1987) and adult populations commonly reach very high density, becoming important biting nuisance pests. Historically, *C. tarsalis* has played a prominent role in the maintenance and transmission of arboviruses including St. Louis Encephalitis Virus and Western Equine Encephalitis Virus. Laboratory studies have revealed that *C. tarsalis* is among the most efficient vectors of WNV known, with high rates of both oral and vertical transmission (Goddard et al. 2002, 2003). *Culex tarsalis* not only feeds primarily on birds (Reisen and Reeves 1987) and is hypothesized to play an important role in WNV amplification, but also feeds opportunistically on mammals (Reisen and Reeves 1987) and is abundant in peridomestic habitats, possibly serving as a bridge vector to humans and domestic animals. Given its broad range, large population sizes, and high capacity for WNV transmission, *C. tarsalis* is likely in part responsible for recent epidemics in western United States including outbreaks in Nebraska, Colorado, Arizona, New Mexico, and California (Hayes et al. 2005).

Studies of field-caught individuals indicate that there is significant spatial and temporal heterogeneity in the ability of *C. tarsalis* to transmit WNV. Northern California populations exhibited higher transovarial and oral transmission than populations in southern California (Goddard et al. 2002, 2003). WNV infection rates also appear to vary at different times of year (Reisen et al. 2006). The extent to

which these observed temporal and spatial differences in WNV transmission are rooted in genetic variation and/or environmental influences is currently unknown. It is possible that part of the variation that *C. tarsalis* exhibits in viral transmissibility is due to genetic differences among populations. However, except for a single allozyme study (Gimnig et al. 1999), little is known about the genetic structure of *C. tarsalis* populations. This study was undertaken to begin characterizing population structure of *C. tarsalis* in the western United States.

We have characterized the genetic structure of *C. tarsalis* populations across a broad geographical range using both mitochondrial and nuclear markers. We conducted a genetic analysis of 12 *C. tarsalis* populations from California, Washington, Colorado, New Mexico, and Nebraska using 5 microsatellite markers and mitochondrial sequence data. Microsatellites revealed moderate genetic structure and isolation by distance, whereas mitochondrial sequences indicated panmixia across the study region. Both types of markers exhibit signatures indicative of a range expansion. Our findings have important implications for future studies on *C. tarsalis* population dynamics, the potential role of genetic structure in explaining variation in viral transmission, and the effect of past evolutionary events on current estimates of gene flow.

## Materials and Methods

### Mosquito Collections and Extractions of DNA

Adult mosquitoes were collected in California, Washington, New Mexico, Colorado, and Nebraska between June and August 2005 using Centers for Disease Control light traps (fig. 1). Specimens were either transported from the collection localities to the Johns Hopkins Bloomberg School of Public Health on dry ice or preserved in 100% ethanol and stored at  $-80^{\circ}\text{C}$  until processed for DNA extraction. Specimens were identified as *C. tarsalis* according to Darsie and Ward (1981). DNA was extracted from individual mosquitoes using the DNeasy Tissue Kit (Qiagen, Valencia, CA) according to Appendix G of the manufacturer's protocol for insects or by salt extraction/ethanol

Key words: *Culex tarsalis*, genetic structure, population expansion, West Nile virus.

E-mail: jrasgon@jhsph.edu.

*Mol. Biol. Evol.* 24(5):1208–1218. 2007

doi:10.1093/molbev/msm040

Advance Access publication March 5, 2007

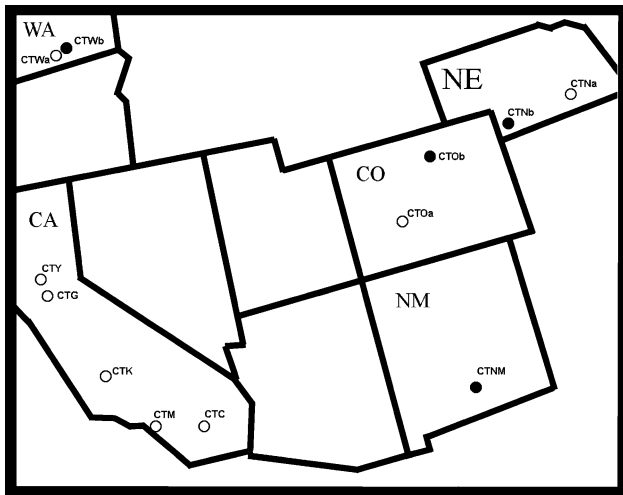


FIG. 1.—Summer 2005 *Culex tarsalis* collection sites. A total of 12 populations were sampled, including 5 in California, 2 each in Colorado, Washington and Nebraska, and 1 in New Mexico. Open circles denote sites where both microsatellite and mitochondrial sequence data were obtained and filled circles denote sites where only microsatellite data were obtained.

precipitation as previously described (Black and DuTeau 1997). Extracted DNA was suspended in nuclease-free water and DNA concentration was quantified using a NanoDrop spectrophotometer (NanoDrop Technologies, Wilmington, DE), adjusted to 25–50 ng/ $\mu$ L, and stored at  $-20^{\circ}$  C until used for Polymerase Chain Reaction (PCR).

#### ND4 Mitochondrial DNA Amplification and Sequencing

A 389 bp fragment of the reduced form of nicotinamide adenine dinucleotide dehydrogenase gene subunit 4 was amplified using primers ND4+ and ND4– as previously described (Gorochotegui-Escalante et al. 2000). Amplifications were carried out using DNA from 25 to 32 individuals from each California population and 16 individuals from 1 population each in Washington, Colorado, and Nebraska, for a total of 8 populations ( $N = 170$ ). PCR conditions were as previously described (Gorochotegui-Escalante et al. 2000). Amplicons were separated by 1% agarose gel electrophoresis, purified from the gel using Qiaquick columns (Qiagen), and sequenced in both directions at the Johns Hopkins Medical Institutes Core Sequencing Facility (Baltimore, MD). Because primer sequences contain degenerate sites, these portions were excluded from sequence analysis.

#### Microsatellite Amplification and Fragment Size Determination

Five trinucleotide repeat microsatellite loci were selected from 12 previously identified markers for analysis (CUTC6, CUTC12, CUTD107, CUTD113, and CUTD120) (Rasgon, Venkatesan et al. 2006). Primer sequences and PCR conditions were as previously described (Rasgon et al. 2006). Amplifications were carried out using DNA from 24 to 38 individuals from each of 12 populations

( $N = 356$ ). Forward primers were 5' labeled with either HEX or 6FAM for marker multiplexing. Labeled amplicons were resolved on an ABI Prism Genetic Analyzer 3100 Avant (Applied Biosystems, Foster City, CA). Allele sizes were automatically estimated with an internal ROX-500 size standard (Applied Biosystems) using GeneScan v. 3.1 and Genotyper software (Applied Biosystems).

#### Diversity and Population Structure Analyses

ND4 haplotype polymorphism and nucleotide diversity, estimated by  $\pi$  (the average number of nucleotide differences per site between 2 sequences, calculated according to Nei (1987), were determined using DnaSP 4.0 (Rozas et al. 2003). Microsatellite allele frequencies were analyzed for deviation from Hardy–Weinberg equilibrium and linkage disequilibrium using Arlequin 2.0 (Schneider et al. 2000) and GenePop software (Raymond and Rousset 1995). Genetic diversity values were not normally distributed, so diversity among populations was compared using the Wilcoxon matched-pairs sign-rank test for microsatellite loci and a Chi-square goodness of fit test for ND4 sequences.

Arlequin 2.0 was used to compute  $F_{ST}$  values (Wright 1951, Weir and Cockerham 1984) and significance determined by permutation tests (1,000 permutations). An unweighted pair group method with arithmetic mean (UP-GMA) phylogenetic tree inferred from microsatellite-derived multilocus  $F_{ST}$  values was constructed using MEGA v. 3.1 (Kumar et al. 2004). Branch lengths were determined using the program PHYLIP (Felsenstein 1989). A statistical parsimony (Templeton et al. 1992) haplotype network of unique ND4 sequences was constructed using the program TCS 1.21 (Clement et al. 2000) with a 95% cutoff.

Structure 2.0 (Pritchard et al. 2000) was used to assign individuals from all populations to a predetermined number of clusters ( $K$ ) based on multilocus microsatellite data. For each run, a burn-in period of 30,000 steps was followed by 1,000,000 iterations under the admixture model and the assumption of correlated allele frequencies among populations ( $\gamma = 0.3468$ , calculated in 5 runs at  $K = 1$ ). For each  $K$  of 1–6, 10 runs were performed. Log-likelihood scores were averaged across runs and compared to determine the posterior probability of each  $K$ . Arlequin 2.0 was used to partition genetic variation among regions of restricted gene flow (based on microsatellite-derived clustering results and  $F_{ST}$  values) using analysis of molecular variance (AMOVA). Regressions of linearized  $F_{ST}$  values on ln-transformed geographic distances among populations (Rousset 1997) were performed for microsatellite and ND4-derived data using STATA 8.0. Mantel probabilities were calculated using IBD 1.52 (Bohonak 2002).

#### Methods to Infer Population Expansion

Several test statistics have been developed to determine whether microsatellite and mitochondrial haplotype frequencies deviate from evolutionary neutrality. These statistics are based on a comparison of observed variability (measured by heterozygosity, haplotype or nucleotide

**Table 1**  
**Summary Statistics of ND4 Sequence Variation in 8 *Culex tarsalis* Populations from the Western United States**

Population	Location	<i>N</i>	<i>H</i>	<i>S</i>	Hd	$\pi$	<i>K</i>	<i>D</i>	<i>r</i>	<i>F<sub>s</sub></i>	<i>S</i>	<i>D</i> *	<i>F</i> *
CTC	Coachella, CA	29	15	18	0.852	0.0066	2.32	-1.81*	0.041	-9.07**	1.00**	-2.25	-2.48
CTM	Los Angeles, CA	26	16	17	0.948	0.0079	2.76	-1.79	0.067	-10.19**	1.00**	-2.06	-2.32
CTK	Kern, CA	23	11	15	0.775	0.0066	2.29	-1.56	0.049	-4.60**	0.997**	-1.71	-1.94
CTG	Yolo, CA	30	17	18	0.913	0.0063	2.21	-1.77	0.047	-12.85**	1.00**	-2.82*	-2.92*
CTY	Yuba, CA	16	9	9	0.858	0.0061	2.14	-0.77	0.047	-3.89*	0.995*	-1.01	-1.09
CTWa	Benton, WA	16	12	13	0.926	0.0069	2.40	-1.43	0.052	-9.94**	1.00**	-1.05	-1.34
CTOa	Gunnison, CO	16	10	10	0.867	0.0050	1.74	-1.57	0.070	-6.50**	1.00**	-1.67	-1.89
CTNa	Adams, NE	14	12	14	0.962	0.0076	2.64	-1.72	0.051	-7.87**	1.00**	-2.17	-2.35
Overall		170	64	49	0.887	0.0068	2.36	-2.29**	0.034	-92.82**	1.00**	-4.67*	-4.37*

NOTE.—*N*, number of sequences analyzed; *H*, number of haplotypes; *S*, number of segregating sites; Hd, haplotype diversity;  $\pi$ , nucleotide diversity; *K*, average number of nucleotide differences; *D*, Tajima's statistic (Tajima 1989); *r*, raggedness statistic (Harpending 1994); *F<sub>s</sub>*, Fu's statistic (Fu 1997); *S*, Strobeck's statistic (Strobeck 1987); *D*\* and *F*\*, Fu and Li's statistics (Fu and Li 1993).

\*  $P < 0.05$ ; \*\*  $P < 0.01$ . Significance was determined using coalescent simulations in DnaSP v. 4.0.

diversity, and number of pairwise differences or segregating sites) to what would be expected under mutation-drift equilibrium or population growth. *H* and *K* tests (Depaulis and Veuille 1999) were performed on ND4 sequence data using the program Allelix (provided by S. Mousset). These tests compare observed haplotype diversity and number with an expected distribution of values under equilibrium conditions. Strobeck's *S* statistic (Strobeck 1987), the probability of having an equal number or fewer haplotypes than observed based on the gene frequency distribution derived from the inferred mutation rate  $\theta$ , was computed for each population using the program DnaSP v. 4.0. Mismatch distributions (Rogers and Harpending 1992, Rogers 1995) and site-frequency spectra (Donnelly et al. 2001) produce characteristic patterns believed to reflect population expansion. Distributions and frequency spectra were plotted across all samples and for each population using DnaSP v. 4.0 along with the corresponding raggedness statistic (Harpending 1994) to quantify the smoothness of mismatch distributions.

Fu and Li's *D*\* and *F*\* (Fu and Li 1993), and Fu's *F<sub>s</sub>* statistics test for deviation of sequence variation from evolutionary neutrality. Fu's *F<sub>s</sub>* is based on the probability of the observed number of haplotypes or greater occurring under conditions of neutrality, whereas Fu and Li's *D*\* and *F*\* compare estimates of theta based on mutations in internal (older) and external (younger) branches of a genealogy. Negative values of these statistics are most often attributed to positive selective sweeps (such as genetic hitchhiking), recent population growth, or background selection. These events may all result in similar sequence patterns such as an excess of rare haplotypes, but different tests exhibit varying levels of sensitivity in detecting potential causes. Used in combination, these tests can provide evidence for or against particular evolutionary mechanisms. Fu and Li's *D*\* and *F*\* and Fu's *F<sub>s</sub>* tests and confidence intervals (CI) calculated from coalescent simulations were conducted using DnaSP v. 4.0.

A multilocus test of expected homozygosity (and conversely heterozygosity) has been developed for microsatellite evolution under a variety of mutation models (Cornuet and Luikart 1996). Expected heterozygosity under Hardy-Weinberg allele frequencies ( $H_{eq}$ ) is compared with expected heterozygosity calculated from the expected number of alleles and sample size ( $H_{eq}$ ). Under conditions of rapid

population growth, high mutation rates and low loss of variation from drift would cause both heterozygosity and allele number to increase, though allele number would increase at a more rapid rate. As a result,  $H_{eq}$  would be greater than  $H_e$  (Cornuet and Luikart 1996), providing a signature of population expansion. Microsatellites generally follow the stepwise mutation model (SMM) or have a small percentage of multistep mutations (2-phase model or TPM) (Weber and Wong 1993, Di Rienzo et al. 1994, Primmer et al. 1998). Tests under strict SMM and TPM with 5%, 10%, and 15% multistep mutations were performed using the program Bottleneck (Cornuet and Luikart 1996).

## Results

### ND4 Haplotype and Nucleotide Polymorphism

Sixty-four ND4 haplotypes were detected in 170 *C. tarsalis* individuals across 8 populations. Forty-nine of 349 nucleotide positions were variable and only 5 substitutions were nonsynonymous. The number of haplotypes per population ranged from 9 to 17, with a mean of 12.75 (table 1). Once haplotype richness was weighted by sample size, no significant differences in haplotype number were observed. Haplotype diversity (Hd) ranged from 0.78 to 0.96 among populations and nucleotide diversity ( $\pi$ ) ranged from 0.0050 to 0.0079. Haplotype diversity (Hd) and nucleotide diversity ( $\pi$ ) did not vary significantly among populations.

*H* and *K* tests indicated that although overall ND4 haplotype diversity did not deviate from the expected distribution (observed Hd = 0.88; 95% CI of expected Hd = 0.81–0.94;  $P = 0.37$ ), the number of observed haplotypes, at 64, is much greater than what would be expected under the neutral model (95% CI of expected number of haplotypes = 16–35;  $P < 0.0001$ ).

### Hardy-Weinberg Equilibrium, Linkage Disequilibrium, and Microsatellite Polymorphism

Significant deviation from Hardy-Weinberg equilibrium was found in 8 of 60 possible tests (Bonferroni adjusted  $\alpha = 0.0008$ ; table 2). All deviations were due to

**Table 2**  
**Sample Size (N), Number of Alleles, and Expected and Observed Heterozygosities ( $H_e$  and  $H_o$ ) of 5 Microsatellite Loci in 12 *C. tarsalis* Populations from the Western United States**

Population	Location	N	Microsatellite Loci					Mean												
			CUTC6		CUTC12		CUTC113		CUTD107		CUTD120									
			Number of alleles	$H_e$	$H_o$	Number of alleles	$H_e$	$H_o$	Number of alleles	$H_e$	$H_o$	Number of alleles	$H_e$							
CTC	Coachella, CA	27	3	0.210	0.111	8	0.794	0.778	4	0.488	0.444	5	0.262	0.260	4	0.510	0.556	4.8	0.453	0.430
CTM	Los Angeles, CA	25	4	0.384	0.240	10	0.824	0.680	4	0.575	0.600	3	0.384	0.333	4	0.744	0.480	5.0	0.582	0.467
CTK	Kern, CA	24	4	0.354	0.000	10	0.834	0.792	4	0.404	0.167*	3	0.541	0.400	5	0.664	0.333	5.2	0.559	0.338
CTG	Yolo, CA	29	4	0.481	0.103*	7	0.822	0.552	5	0.460	0.345	3	0.425	0.143*	5	0.629	0.517	4.8	0.563	0.332
CTY	Yuba, CA	32	5	0.262	0.094*	7	0.732	0.563	6	0.633	0.656	6	0.479	0.344	5	0.643	0.469	5.2	0.550	0.425
CTWA	Benton, WA	30	4	0.394	0.200	8	0.802	0.767	6	0.565	0.500	3	0.129	0.100	6	0.623	0.200*	5.4	0.503	0.353
CTWB	Benton, WA	38	3	0.092	0.063	10	0.787	0.688*	6	0.384	0.344	4	0.207	0.125	6	0.694	0.313*	5.8	0.433	0.306
CTNM	Otero, NM	30	4	0.245	0.167	8	0.536	0.467	7	0.736	0.714	4	0.421	0.333	6	0.660	0.567	5.8	0.520	0.450
CTOA	Gunnison, CO	32	3	0.185	0.097	10	0.840	0.688*	7	0.577	0.531	4	0.403	0.452	5	0.695	0.258*	5.8	0.540	0.405
CTOB	Boulder, CO	27	4	0.242	0.185	6	0.795	0.593	7	0.626	0.482	4	0.184	0.154	5	0.720	0.385	5.2	0.514	0.360
CTNA	Adams, NE	32	3	0.122	0.094	8	0.713	0.594	6	0.694	0.625	5	0.285	0.188	6	0.673	0.563	5.6	0.497	0.413
CTNB	Chase, NE	32	3	0.122	0.094	7	0.704	0.656	7	0.652	0.625	3	0.286	0.219	7	0.683	0.563	5.4	0.489	0.431

\* $P < 0.05$  (Bonferroni corrected  $\alpha$ ).

heterozygosity deficiency. None of the pairs of loci exhibited significant linkage disequilibrium (Bonferroni corrected  $\alpha = 0.0004$ ) in single pairwise tests. Fisher's global test for each pair of loci across all 12 populations also did not reveal significant linkage disequilibrium.

The 5 microsatellite loci had an average of 5.3 alleles per locus per population and ranged between 3 and 10 alleles in each population. Average heterozygosity per locus ranged between 0.12 and 0.71. No significant differences in allele number or heterozygosity were detected among populations.

### Phylogenetic Analyses

An ND4 haplotype network was constructed using statistical parsimony with a 95% connection limit (parsimony cutoff = 7 mutational steps) (fig. 2). Approximately 1/3 of the individuals in each population shared haplotype X, which is inferred to be the ancestral haplotype (fig. 2). A star-like pattern of closely related haplotypes appeared to radiate from haplotype X. Of the remaining 63 haplotypes, 47 were unique, occurring in only one individual from the entire sample. Geographic clustering of haplotypes was not observed.

Population pairwise  $F_{ST}$  values based on microsatellite allele frequencies were used to generate a UPGMA population phylogeny, in which a constant rate of evolution across populations is assumed and genetic distances between populations are relative. Based on an  $F_{ST}$  cutoff of 0.05, considered to represent moderate genetic isolation (Wright 1978), 3 population clusters are present. These include 1) 4 California populations (CTM, CTG, CTY, and CTK) along with Colorado and Washington (CTOa, CTOb, CTWa, and CTWb), 2) New Mexico (CTNM) and Nebraska (CTNa and CTNb), and 3) population CTC in California (fig. 3). Population pairwise  $F_{ST}$  values based on ND4 haplotype frequencies ranged from 0.00 to 0.008. Because pairwise ND4  $F_{ST}$  values were very low and nonsignificant, a phylogenetic tree constructed from these data is not presented here.

### Population Genetic Structure

The posterior probability for  $K = 3$  clusters in the microsatellite-based multilocus clustering analysis was 0.95. Posterior probabilities for  $K = 1, 2,$  and  $4-6$  were nearly 0. At  $K = 3$ , population CTC (Coachella, CA) appeared to be distinct, as did the cluster of CTNM, CTNa, and CTNb (fig. 3), corroborating results from the  $F_{ST}$ -based UPGMA tree. The remaining populations appear to share similar proportions of ancestry from each of the other 2 groups as well as from a 3rd group. In all cases, high levels of admixture were present within groups and individuals.

Microsatellite-based phylogenetic and cluster analyses were used to designate 3 genetically distinct groups of populations (fig. 3). An AMOVA conducted by partitioning variation among and within groups and populations revealed that ND4 haplotype variation was attributed solely to within-population differences (100%) and not to differences among populations or the 3 geographic regions delineated by microsatellite-derived genetic distances

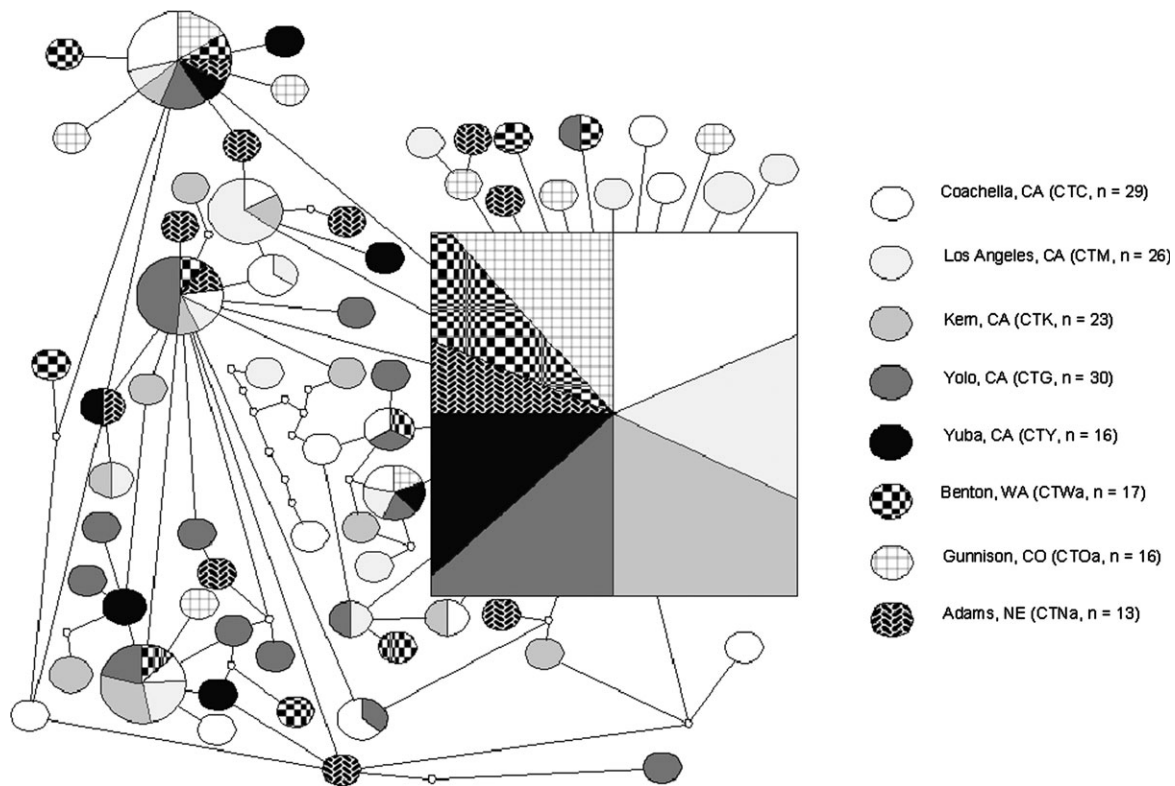


FIG. 2.—Statistical-parsimony haplotype network with 95% cutoff, inferred from ND4 sequence variation in 8 populations. Each node represents one nucleotide difference. Empty circles indicate inferred haplotypes. Oval or square size is proportional to haplotype frequency.

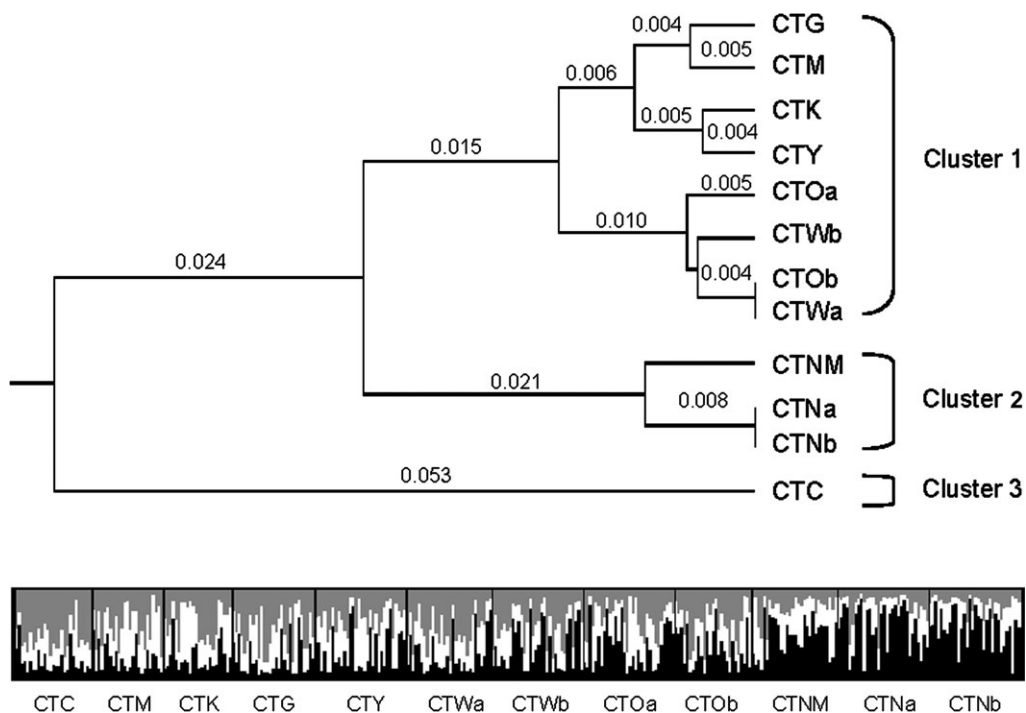


FIG. 3.—Microsatellite-based clustering analyses. Top panel: UPGMA tree inferred from multilocus microsatellite-derived pairwise  $F_{ST}$  values. Brackets indicate possible genetic clustering of 3 groups based on cutoff of  $F_{ST} = 0.05$ . Genetic distance between Cluster 1 and Cluster 2,  $F_{ST} = 0.060$ ; between Cluster 2 and Cluster 3,  $F_{ST} = 0.098$ ; between Cluster 1 and Cluster 3,  $F_{ST} = 0.092$ . Bottom panel: Plot from microsatellite-based structure analysis at  $K = 3$ . Each individual is represented by a vertical bar displaying membership coefficients to each of 3 clusters, depicted as white, gray, and black. Individuals are grouped by collection site.

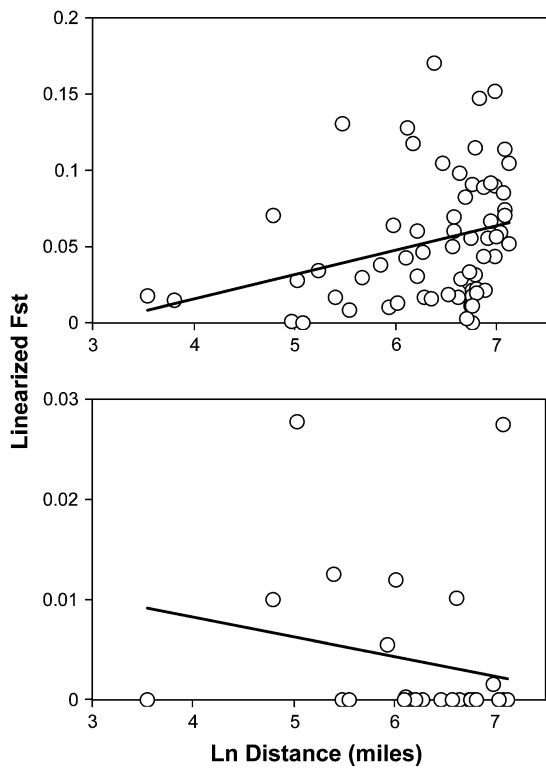


FIG. 4.—Mantel tests for isolation by distance. Top panel: Regression based on microsatellite-derived  $F_{ST}$  values among 12 populations. Regression slope =  $0.054 \pm 0.007$ .  $R^2 = 0.084$ . Mantel probability  $P < 0.004$ . Bottom panel: Regression based on ND4-derived  $F_{ST}$  values among 8 populations. Regression slope =  $-0.002 + 0.002$ .  $R^2 = 0.043$ . Mantel probability  $P = 0.81$ .

( $F_{CT} = -0.002$ ,  $P = 0.45$ ). In contrast, the microsatellite-based AMOVA indicated that 93% of observed variation in microsatellites was attributed to within-population differences. Approximately 6% of the variation in microsatellite allele frequencies was associated with differences among the 3 regions ( $F_{CT} = 0.055$ ,  $P < 0.001$ ), whereas the remaining variation (<2%) was attributed to among-population differences ( $F_{ST} = 0.073$ ,  $P < 0.001$ ).

Gene Flow among Populations

The Mantel regression for ND4 sequence data (fig. 4) did not yield a significant relationship between genetic and geographic distance (Mantel probability  $P = 0.823$ ). The Mantel regression of linearized microsatellite  $F_{ST}$  values on the natural logarithm of pairwise distances among collection sites (fig. 4) revealed isolation by distance. The relationship was positive (slope = 0.054;  $R^2 = 0.084$ ) and statistically significant (Mantel probability  $P < 0.004$ ).

Pairwise  $F_{ST}$  values for ND4 haplotype data ranged from 0.000 to 0.027, yielding estimated  $N_m$ 's of 17.73 to infinity. Pairwise ND4  $F_{ST}$  values were not significantly different among any of the populations. Mean pairwise  $F_{ST}$  values for microsatellite allele frequencies ranged from 0.000 to 0.146 resulting in  $N_m$  (estimated number of migrants between populations per generation) values between

**Table 3**  
**Microsatellite-Derived Pairwise Genetic Differentiation ( $F_{ST}$ ) and Net Number of Migrants ( $N_m$ ) among 12 *C. tarsalis* Populations in California, Washington, Colorado, New Mexico, and Nebraska**

	Coachella, CA	Los Angeles, CA	CTM	Kern, CA	CTG	Yolo, CA	CTK	Yuba, CA	CTY	Benton, WA	CTWa	Benton, WA	CTWb	Alamogordo, NM	CTNM	Gunnison, CO	CTOa	Boulder, CO	CTOb	Adams, CO	CTNa	Chase, NE	CTNb	
Coachella, CA	CTC																							
Los Angeles, CA	0.066 <sup>b</sup>	CTM																						
Kern, CA	0.113*	0.010	CTG																					
Yolo, CA	0.115*	0.027	0.016	CTK																				
Yuba, CA	0.105*	0.013	0.017	0.008	CTY																			
Benton, WA	0.103*	0.021	0.017	0.056*	0.029	CTWa																		
Benton, WA	0.083*	0.033	0.044*	0.048*	0.030*	0.015	CTWb																	
Otero, NM	0.146*	0.065*	0.082*	0.076*	0.021	0.066*	0.078*	CTNM																
Gunnison, CO	0.095*	0.017	0.025	0.028	0.018	0.019	0.011	0.06*	CTOa															
Boulder, CO	0.089*	0.011	0.030	0.030	0.022	0.000	0.003	0.057*	0.001	CTOb														
Adams, NE	0.132*	0.069*	0.095*	0.102*	0.049*	0.056*	0.053*	0.015	0.041*	0.037*	CTNa													
Chase, NE	0.128*	0.063*	0.083*	0.084*	0.042*	0.052*	0.042*	0.018	0.029	0.033	0.000	CTNb												

<sup>a</sup> Upper corner:  $N_m$  (number of migrants per generation) estimated from  $F_{ST}$  values.

<sup>b</sup> Lower corner: Pairwise  $F_{ST}$  values.

\*  $P < 0.001$  using Bonferroni adjusted  $\alpha$ . Significance was determined by permutation testing (1,000 permutations; Arlequin v. 2.0).

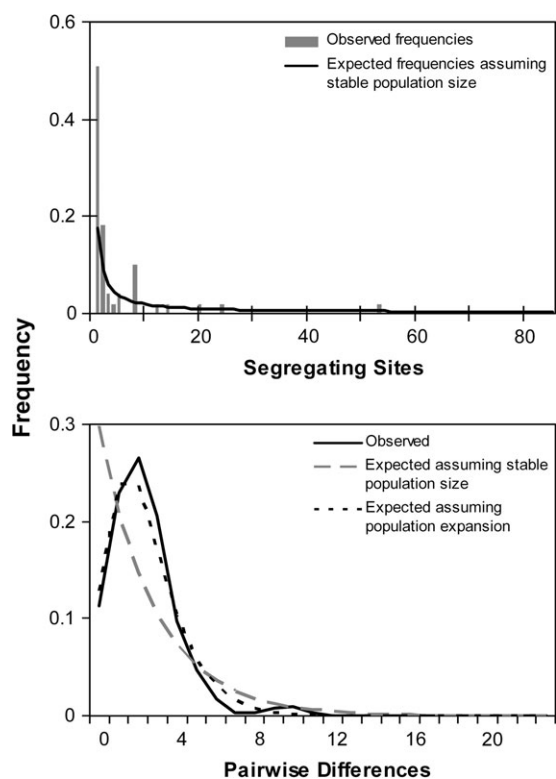


FIG. 5.—Population expansion signatures in mitochondrial ND4 sequence data. Top panel: Mismatch distribution of observed frequencies of pairwise differences among ND4 sequences and expected frequencies under the neutral model of evolution given the null hypothesis of 1) no population change and 2) population expansion. Bottom panel: Site-frequency spectrum indicating excess of singleton mutations in ND4 sequence. Spectrum compares observed frequencies of segregating sites to expected distribution under the null hypothesis of no population change.

1.5 and infinity among populations (table 3). Markov chain pairwise exact tests (Goudet et al. 1996) revealed significant differences between population CTC (Coachella, CA) and all other populations including neighboring population CTM (Los Angeles, CA). Both Nebraska populations (CTNa and CTNb) were genetically distinct from populations in all other states except for CTNM in Otero City, New Mexico. Patterns in pairwise  $F_{ST}$  values were consistent with population structure based on AMOVA and multi-locus clustering analyses.

#### Evolutionary Neutrality and Population Expansion

The mismatch distribution of pairwise nucleotide differences among ND4 sequences among all populations exhibited a smooth unimodal distribution characteristic of a large population expansion (Slatkin and Hudson 1991, Rogers and Harpending 1992) (fig. 5). Similar patterns were observed in the individual distributions for each population except for CTK, which exhibited a more ragged distribution (data not shown). The raggedness statistic  $r$  (Harpending 1994) was lower than expected under conditions of constant growth ( $P(r < 0.0336) = 0.088$ ). Study-wide site-frequency spectra reveal an excess of singleton

mutations when compared with expected frequencies under neutrality and stable population size (fig. 5). Population-specific spectra produced similar patterns (data not shown).

Fu's  $F_s$  was negative ( $F_s = -92.81$ ;  $P < 0.0001$ ) which occurs when an excess of rare haplotypes is present and suggests that either population expansion or genetic hitchhiking has taken place (Fu 1997). Fu and Li's  $D^*$  and  $F^*$  were negative as well ( $D^* = -4.68$ ;  $P < 0.02$ ;  $F^* = -4.38$ ;  $P < 0.02$ ), indicating an excess of recently derived haplotypes and suggesting that either population expansion or background selection has occurred (Fu and Li 1993). Strobeck's  $S$ , the probability of obtaining equal or fewer haplotypes based on gene frequency and mutation rate was very high in all populations, ranging from 0.995 to 1.000. These results are consistent with deviation from neutrality due to either selection or population expansion.

We tested for signatures of population expansion in microsatellites using the heterozygosity test assuming 2 alternative models of microsatellite evolution. Both models gave results with qualitatively similar trends. Under the SMM, assuming that only single-repeat mutations occur, expected heterozygosity based on the number of alleles and sample size ( $H_{eq}$ ) was significantly higher than expected heterozygosity based on allele frequencies ( $H_e$ ) in 10 of the 12 populations (table 4) Under the TPM, assuming that most mutations are single repeats but multistep mutations occur at a frequency of 5%, 10%, or 15%, the number of populations with significant excesses in  $H_{eq}$  fell to 9, 8 and 6 of 12 populations, respectively. All populations with significant  $H_{eq} > H_e$  exhibited this excess for at least 4 of the 5 loci.

The date of the population growth event in mutational time, or  $\tau$ , was calculated to be 1.285  $\mu$  generations, where  $\mu$  is the sequence's mutation rate per generation. Calculation of  $\tau$  was based on the average number of pairwise differences among ND4 sequences (DnaSP v. 4.0). We used this value to estimate the approximate timing of the population expansion by the equation  $\tau = 2\mu t$  (Slatkin and Hudson 1991), where  $\mu$  was conservatively estimated as  $5.7 \times 10^{-8}$  substitutions/site/year (Tamura 1992) and  $t$  is time in generations. Solving for  $t$ ,  $t = \tau/2\mu = 1.285/(2 \times 5.7 \times 10^{-8}) = 11,271,930$  generations. Assuming an average of 20–30 generations per year, we estimate that the population expansion occurred approximately 375,000–560,000 years ago. This date range should be regarded as preliminary due to the small size of the analyzed sequence and rough estimation of the gene's mutation rate.

#### Discussion

Sequence analysis of the ND4 mitochondrial DNA fragment from *C. tarsalis* populations across 4 states revealed a lack of isolation by distance, genetic structuring, and clustering of haplotypes by population or geographic region. Taken alone, ND4 results suggest that either: 1) current gene flow is very high across a large geographic range, 2) *C. tarsalis* experienced a selective mitochondrial sweep, or 3) *C. tarsalis* underwent an expansion that genetically homogenized populations after which there has been insufficient time for signatures of mitochondrial

**Table 4**  
**Heterozygosity Test for Signatures of Population Expansion in 5 Microsatellite Loci in 12 *C. tarsalis* Populations in California, Washington, Colorado, New Mexico, and Nebraska**

		California					Washington		New Mexico	Colorado		Nebraska	
		CTC	CTM	CTG	CTK	CTY	CTWa	CTWb	CTNM	CTOa	CTOb	CTNa	CTNb
SMM	$H_{eq} > H_e$	5/5*	4/5	4/5*	4/5*	5/5*	5/5*	4/5*	5/5*	5/5*	3/5	5/5*	5/5*
	Mean SD	-2.30	-1.06	-1.09	-1.77	-1.79	-2.14	-2.99	-2.18	-2.13	-2.59	-2.62	-2.85
	S.E.	(2.26)	(1.55)	(1.35)	(1.80)	(2.35)	(1.13)	(2.09)	(1.74)	(1.82)	(2.84)	(1.79)	(1.41)
TPM, 95%	$H_{eq} > H_e$	5/5*	4/5	4/5	4/5*	5/5*	4/5*	4/5*	5/5*	4/5*	3/5	5/5*	5/5*
	Mean SD	-1.85	-0.76	-0.85	-1.39	-1.32	-1.69	-2.51	-1.75	-1.74	-2.04	-1.93	-2.38
	SE	(1.87)	(1.32)	(1.26)	(1.58)	(1.84)	(1.07)	(1.92)	(1.43)	(1.63)	(2.49)	(1.51)	(1.37)
TPM, 90%	$H_{eq} > H_e$	4/5*	3/5	4/5	4/5*	4/5*	4/5*	4/5*	5/5*	3/5	3/5	5/5*	5/5*
	Mean SD	-1.64	-0.63	-0.65	-1.26	-1.10	-1.50	-2.23	-1.41	-1.43	-1.79	-1.80	-1.98
	SE	(1.91)	(1.27)	(1.17)	(1.59)	(1.86)	(1.03)	(1.85)	(1.20)	(1.47)	(2.36)	(1.53)	(1.30)
TPM, 85%	$H_{eq} > H_e$	4/5*	3/5	4/5	4/5	3/5	4/5*	4/5*	5/5*	3/5	3/5	5/5*	5/5*
	Mean SD	-1.43	-0.49	-0.50	-1.03	-1.00	-1.27	-2.01	-1.23	-1.25	-1.55	-1.57	-1.77
	SE	(1.71)	(1.15)	(1.06)	(1.44)	(1.82)	(1.98)	(1.75)	(1.10)	(1.43)	(1.24)	(1.46)	(1.25)

NOTE.—Fractions indicate number of loci (out of 5) with  $H_{eq} > H_e$ . Mean SD and SE are mean standardized deviations from equilibrium heterozygosity along with associated standard error.  $s^2 = 30$  for all TPMs.

\* Statistically significant  $H_{eq}$  excess (1-tailed Wilcoxon rank-sum test;  $P < 0.05$ ).

population structure to be detected. Previous allozyme data (Ginnig et al. 1999) and our microsatellite results suggest that populations are not panmictic across the collection range, refuting the 1st hypothesis. Evidence for selective mitochondrial sweeps in conjunction with invasion of maternally inherited *Wolbachia* endosymbionts have been observed in the congeneric *Culex pipiens* species complex (Rasgon, Cornel, Scott 2006), but because *C. tarsalis* is not infected with *Wolbachia* (Rasgon and Scott 2004) hypothesis 2 is not a likely explanation of our results.

The most likely explanation for our observations is that *C. tarsalis* underwent a population expansion some time in the relatively recent past. Statistical signatures of population expansion are detectable in both ND4 and microsatellite data. ND4 statistical parsimony analysis shows a star-shaped phylogeny (Slatkin and Hudson 1991) and a large number of rare haplotypes separated by single-nucleotide differences.  $H$  and  $K$  tests, Strobeck's  $S$  statistics, and site-frequency spectra were consistent with the presence of a rapidly growing population, whereas mismatch distributions indicated that a single or few haplotypes spread and mutated to generate several closely related haplotypes, as is often observed during population expansion (Rogers and Harpending 1992). Fu's  $F_s$  and Fu and Li's  $D^*$  and  $F^*$  all indicated a significant negative deviation from evolutionary neutrality. Though it is impossible to distinguish between selection and expansion as the cause of negative  $F_s$ ,  $D^*$ , and  $F^*$  values, these statistics in combination with our microsatellite data are indicative of a deviation from equilibrium which was likely caused by population expansion.

Several populations demonstrated an excess in expected microsatellite heterozygosity based on microsatellite allele number ( $H_{eq}$ ) when compared with expected heterozygosity based on allele frequencies ( $H_e$ ), which occurs under conditions of rapid population growth (Cornuet and Luikart 1996). Heterozygote excess based on allele number

was most pronounced under the SMM, though populations exhibited moderate to widespread  $H_{eq}$  excess and no significant deficiencies across all models tested, providing corroborative evidence of population expansion. An alternate explanation for  $H_{eq} > H_e$  is the influx of rare alleles from genetically distinct populations (Cornuet and Luikart 1996). This phenomenon is unlikely because multiple populations over a large geographic range demonstrated the same pattern.

Our results represent an example of how current estimates of gene flow, particularly those based on mitochondrial sequences, may be exaggerated due to past events such as range expansion. Evidence of population expansion has recently been found in many disease vectors including *Triatoma infestans*, *Amblyomma americanum*, *Anopheles funestus*, *Anopheles darlingi*, *Simulium tani*, *Anopheles gambiae*, and *A. dirus* (Walton et al. 2000, Donnelly et al. 2001, Pramual et al. 2005, Barges et al. 2006, Michel et al. 2006, Mirabello and Conn 2006, Mixson et al. 2006), suggesting that it may not be an uncommon phenomenon in arthropods. Because both extensive gene flow and range expansion can produce similar patterns in mitochondrial sequence data, lack of isolation by distance and significant partitioning of variance among groups or populations may not necessarily be indicative of current panmixia. Instead, they may reflect historical events and should be interpreted carefully.

ND4 sequences suggest that the expansion of *C. tarsalis* in the western United States occurred between 375,000 and 560,000 years ago. Other studies of *Anopheles* population dynamics have suggested that range expansions in Africa and Asia may be associated with changes in agricultural practices (Walton et al. 2000, Donnelly et al. 2001). Our estimate predates human civilization and the development of agriculture in North America by well over 300,000 years, suggesting that the expansion was likely not influenced by anthropogenic forces. Instead, it is more



likely to have been associated with climatic changes such as the Nebraskan or Kansan stages of Pleistocene glaciation (Dreeszen 1970) that occurred in the midwestern and western United States between 350,000 and 1 MYA.

Microsatellites in our study reflected both signatures of population expansion (nonequilibrium conditions) and isolation by distance (consistent with evolutionary equilibrium). Microsatellites have been shown to have higher rates of mutation than mitochondrial genes, ranging in insects and mammals from  $10^{-3}$  to  $10^{-6}$  mutations per locus per generation (Dietrich et al. 1992; Edwards et al. 1992; Weber and Wong 1993; Schug et al. 1997, 1998), whereas mitochondrial gene mutation rates have been estimated at  $9.4 \times 10^{-8}$  substitutions per 4-fold degenerate site in mammals (Brown et al. 1982) and at  $5.7 \times 10^{-8}$  substitutions in *Drosophila* species (Tamura 1992). The discrepancy between microsatellite and mitochondrial-derived genetic structure may be attributed to the fact that after range expansion rapidly mutating microsatellites have begun to differentiate among populations, whereas the more slowly mutating mitochondrial gene does not reflect the presence of genetically isolated populations.

Microsatellite-based population structure did not appear to be associated with major geographic features such as the Cascade, Sierra Nevada, or Rocky Mountain ranges. The Tehachapi Mountain range has previously been associated with genetic structure among southern California *C. tarsalis* populations (Gimnig et al. 1999). Although we observed that populations south of the Tehachapis (CTC and CTM) were genetically distinct from each other, the divergence did not seem to be associated with this mountain range. Interestingly, although the 2 Nebraska populations appeared to be panmictic and cluster with New Mexico, they were genetically distinct from both Colorado populations, which fall on either side of the Rocky Mountains. These results suggest that there may be a barrier to gene flow between the 2 neighboring states that is not associated with the Rockies. The arid Great Plains, which ranges across eastern Colorado and New Mexico to Iowa, may limit migration between populations in Colorado and Nebraska.

Generally, patterns of gene flow inferred from microsatellite data exhibit isolation by distance and geographical clustering but are not sufficiently explained by topographical barriers or geographic distance alone. This phenomenon may result from an insufficient number of loci, movement of mosquitoes based on agricultural practices or other environmental features beyond distance and elevation, or residual effects of range expansion. The inclusion of more loci and populations from as yet unsampled regions will likely address the first 2 possibilities. Regardless, it is still likely that microsatellites reflect only a partial return to evolutionary equilibrium after the expansion event because they exhibit signatures of both equilibrium and nonequilibrium conditions. The fact that microsatellites may underestimate current levels of genetic isolation among populations in the western United States should be taken into account when gathering and interpreting further information on the genetic structure of *C. tarsalis*.

*Culex tarsalis* is known to exhibit significant spatial and temporal heterogeneity in a variety of phenotypic traits

including autogeny, feeding behavior, and vertical and horizontal arboviral transmission. Thus far, genetic and environmental determinants of such phenotypic variation, including WNV transmission, are largely unknown. Although our findings of microsatellite-based genetic structure may not reflect the full extent of reproductive isolation across the western United States, they are indicative of significant genetic differentiation among mosquito populations and thus allow for the possibility of a relationship between genetic and spatial variation in WNV vector competence. Genetic determinants of vector–pathogen interactions have been identified in several other systems by quantitative trait locus (QTL) analysis, including transovarial transmission of LaCrosse virus in *Ochlerotatus triseriatus*, midgut infection and escape of dengue virus in *Aedes aegypti*, and *Plasmodium* resistance in *A. gambiae* (Bosio et al. 2000, Graham et al. 2003, Zheng et al. 2003, Gomez-Machorro et al. 2004). Recently, *Plasmodium* resistance was mapped in naturally occurring populations of *A. gambiae* in Kenya (Menge et al. 2006) and Mali (Riehle et al. 2006). QTL analyses such as these may lay the foundation for developing biomarkers of vector susceptibility and novel targets for genetic manipulation and disease control. Future studies on genetic and phenotypic spatial variation of *C. tarsalis* will provide the foundation for understanding genetic determinants of viral susceptibility and disease transmission in this important arboviral vector.

### Supplementary Material

The sequence data for this paper appear in GenBank under accession numbers EF125799–EF125862.

### Acknowledgments

We thank W. K. Reisen for kindly providing colony and field specimens. We thank H. Lothrop, D. Lemenager, A. Moser, M. Weissman, M. DiMenna, W. L. Kramer, and M. Stromer for providing field collections. This work was funded by National Institute of Environmental Health Sciences Training Grant T32 ES07141, National Institutes of Health Grant R01AI067371 and the Johns Hopkins Malaria Research Institute. Research conducted at The W. Harry Feinstone Department of Molecular Microbiology and Immunology, Bloomberg School of Public Health, Johns Hopkins University, Baltimore, MD.

### Literature Cited

- Bargues MD, Klisiowicz DR, Panzera F, et al. (14 co-authors). 2006. Origin and phylogeography of the chagas disease main vector *Triatoma infestans* based on nuclear rDNA sequences and genome size. *Infect Genet Evol.* 6:46–62.
- Bell JA, Mickelson NJ, Vaughan JA. 2005. West Nile virus in host-seeking mosquitoes within a residential neighborhood in Grand Forks, North Dakota. *Vector Borne Zoonotic Dis.* 5:373–382.
- Black WCI, DuTeau NM. 1997. RAPD-PCR and SSCP analysis for insect population genetic studies. In: Crampton JM, Beard

- CB, Louis C, editors. The molecular biology of insect disease vectors. Cambridge: Cambridge University Press. p. 361–373.
- Bohonak AJ. 2002. IBD (isolation by distance): a program for analyses of isolation by distance. *J Hered.* 93:153–154.
- Bosio CF, Fulton RE, Salasek ML, Beaty BJ, Black WC. 2000. Quantitative trait loci that control vector competence for dengue-2 virus in the mosquito *Aedes aegypti*. *Genetics.* 156:687–698.
- Brown WM, Prager EM, Wang A, Wilson AC. 1982. Mitochondrial DNA sequences of primates: tempo and mode of evolution. *J Mol Evol.* 18:225–239.
- Clement M, Posada D, Crandall KA. 2000. TCS: a computer program to estimate gene genealogies. *Mol Ecol.* 9:1657–1660.
- Cornuet JM, Luikart G. 1996. Description and power analysis of two tests for detecting recent population bottlenecks from allele frequency data. *Genetics.* 144:2001–2014.
- Darsie RF, Ward RA. 1981. Identification and geographical distribution of the mosquitoes of North America, north of Mexico. *Mosq Syst. Suppl.* 1:1–313.
- Depaulis F, Veuille M. 1999. Neutrality tests based on the distribution of haplotypes under an infinite-site model. *Mol Biol Evol.* 15:1788–1790.
- Dietrich W, Katz H, Lincoln SE, Shin H-S, Friedman J, Dracopoli NC, Lander ES. 1992. A genetic map of the mouse suitable for typing intraspecific crosses. *Genetics.* 131:423–447.
- DiMenna MA, Bueno R Jr, Parmenter RA, Norris DE, Sheyka JM, Molina JL, LaBeau EM, Hatton ES, Glass GE. 2006. Emergence of West Nile virus in mosquito (Diptera: Culicidae) communities of the New Mexico Rio Grande Valley. *J Med Entomol.* 43:594–599.
- Di Rienzo A, Peterson AC, Garza JC, Valdes AM, Slatkin M, Freimer NB. 1994. Mutational processes of simple-sequence repeat loci in human populations. *Proc Natl Acad Sci USA.* 91:3166–3170.
- Donnelly MJ, Licht MC, Lehmann T. 2001. Evidence for recent population expansion in the evolutionary history of the malaria vectors *Anopheles arabiensis* and *Anopheles gambiae*. *Mol Biol Evol.* 18:1353–1364.
- Dreeszen VH. 1970. The stratigraphic framework of Pleistocene glacial and periglacial deposits in the Central Plains. In: Dort W Jr, Jones JK Jr, editors. Pleistocene and recent environments of the Central Great Plains. Kansas City (KS): University Press of Kansas. p. 9–22.
- Edwards A, Hammond HA, Jin L, Caskey CT, Chakraborty R. 1992. Genetic variation at five trimeric and tetrameric tandem repeat loci in four human population groups. *Genomics.* 12:241–253.
- Felsenstein J. 1989. PHYLIP—phylogeny inference package (Version 3.2). *Cladistics.* 5:164–166.
- Fu Y-X. 1997. Statistical tests of neutrality of mutations against population growth, hitchhiking and background selection. *Genetics.* 147:915–925.
- Fu Y-X, Li W-H. 1993. Statistical tests of neutrality of mutations. *Genetics.* 133:693–709.
- Gimnig JE, Reisen WK, Eldridge BF, Nixon KC, Schutz SJ. 1999. Temporal and spatial genetic variation within and among populations of the mosquito *Culex tarsalis* (Diptera: Culicidae) from California. *J Med Entomol.* 36:23–29.
- Goddard LB, Roth AE, Reisen WK, Scott TW. 2002. Vector competence of California mosquitoes for West Nile virus. *Emerg Infect Dis.* 8:1385–1391.
- Goddard LB, Roth AE, Reisen WK, Scott TW. 2003. Vertical transmission of West Nile virus by three California *Culex* (Diptera: Culicidae) species. *J Med Entomol.* 40:743–766.
- Gomez-Machorro C, Bennett KE, de Lourdes Munoz M, Black WC. 2004. Quantitative trait loci affecting dengue midgut infection barriers in an advanced intercross line of *Aedes aegypti*. *Insect Mol Biol.* 13:637–648.
- Gorochotegui-Escalante N, Munoz ML, Fernandez-Salas I, Beaty BJ, Black WC 4th. 2000. Genetic isolation by distance among *Aedes aegypti* populations along the northeastern coast of Mexico. *Am J Trop Med Hyg.* 62:200–209.
- Goudet J, Raymond M, de Meeüs T, Rousset F. 1996. Testing differentiation in diploid populations. *Genetics.* 144:1933–1940.
- Graham DH, Holmes JL, Beaty BJ, Black WC. 2003. Quantitative trait loci conditioning vertical transmission of La Crosse virus in the eastern treehole mosquito, *Ochlerotatus triseriatus*. *Insect Mol Biol.* 12:307–318.
- Harpending HC. 1994. Signature of ancient population growth in a low-resolution mitochondrial DNA mismatch distribution. *Hum Biol.* 66:591–600.
- Hayes EB, Komar N, Nasci RS, Montgomery SP, O’Leary DR, Campbell GL. 2005. Epidemiology and transmission dynamics of West Nile virus disease. *Emerg Infect Dis.* 11:1167–1173.
- Kumar S, Tamura K, Nei M. 2004. MEGA3: integrated software for molecular evolutionary genetics analysis and sequence alignment. *Brief Bioinform.* 5:150–163.
- Menge DM, Zhong D, Guda T, Gouagna L, Githure J, Beier J, Yan G. 2006. Quantitative trait loci controlling refractoriness to *Plasmodium falciparum* in natural *Anopheles gambiae* mosquitoes from a malaria-endemic region in western Kenya. *Genetics.* 173:235–241.
- Michel AP, Grushko O, Guelbeogo WM, Lobo NF, Sagnon N, Constantini C, Besansky NJ. 2006. Divergence with gene flow in *Anopheles funestus* from the Sudan Savanna of Burkina Faso, West Africa. *Genetics.* 173:1389–1395.
- Mirabello L, Conn JE. 2006. Molecular population genetics of the malaria vector *Anopheles darlingi* in Central and South America. *Heredity.* 96:311–321.
- Mixson TR, Lydy SL, Dasch GA, Real LA. 2006. Inferring the population structure and demographic history of the tick, *Amblyomma americanum* Linnaeus. *J Vector Ecol.* 31:181–192.
- Nei M. 1987. Molecular evolutionary genetics. New York: Columbia University Press.
- Pramual P, Kuvangkadilok C, Baimai V, Walton C. 2005. Phylogeography of the black fly *Simulium tani* (Diptera: Simuliidae) from Thailand as inferred from mtDNA sequences. *Mol Ecol.* 14:3989–4001.
- Primmer CR, Saino N, Møller AP, Ellegren H. 1998. Unraveling the processes of microsatellite evolution through analysis of germ line mutations in barn swallows *Hirundo rustica*. *Mol Biol Evol.* 15:1047–1054.
- Pritchard JK, Stephens M, Donnelly P. 2000. Inference of population structure using multilocus genotype data. *Genetics.* 155:945–959.
- Rasgon JL, Cornel AJ, Scott TW. 2006. Evolutionary history of a mosquito endosymbiont revealed through mitochondrial hitchhiking. *Proc Biol Sci.* 273:1603–1611.
- Rasgon JL, Scott TW. 2004. An initial survey for *Wolbachia* (Rickettsiales: Rickettsiaceae) infections in selected California mosquitoes (Diptera: Culicidae). *J Med Entomol.* 36:23–29.
- Rasgon JL, Venkatesan M, Westbrook CJ, Hauer CM. 2006. Polymorphic microsatellite loci from the West Nile virus vector *Culex tarsalis*. *Mol Ecol Notes.* 6:680–682.
- Raymond M, Rousset F. 1995. GenePop, version 1.2. A population genetics software for exact tests and ecumenicism. *J Hered.* 26:248–249.
- Reisen WK, Fang Y, Martinez VM. 2006. Effects of temperature on the transmission of West Nile virus by *Culex tarsalis* (Diptera: Culicidae). *J Med Entomol.* 43:309–317.

- Reisen WK, Lothrop H, Chiles R, Madon M, Cossen C, Woods L, Husted S, Kramer V, Edman J. 2004. West Nile virus in California. *Emerg Infect Dis.* 10:1369–1378.
- Reisen WK, Reeves WC. 1987. Bionomics and ecology of *Culex tarsalis* and other potential mosquito vector species. In: Reeves WC, editor. *Epidemiology and control of mosquito-borne arboviruses in California, 1943-1987*. Sacramento (CA): California mosquito and vector control association. p. 254–329.
- Riehle MM, Markianos K, Niare O, et al. (15 co-authors). 2006. Natural malaria infection in *Anopheles gambiae* is regulated by a single genomic control region. *Science.* 312:577–579.
- Rogers AR. 1995. Genetic evidence for a Pleistocene population explosion. *Evolution.* 49:608–615.
- Rogers AR, Harpending H. 1992. Population growth makes waves in the distribution of pairwise genetic differences. *Mol Biol Evol.* 9:552–569.
- Rousset F. 1997. Genetic differentiation and estimation of gene flow from F-statistics under isolation by distance. *Genetics.* 145:1219–1228.
- Rozas J, Sanchez-Delbarrio JC, Rozas R. 2003. DnaSP, DNA polymorphism analyses by the coalescent and other methods. *Bioinformatics.* 19:2496–2497.
- Schneider S, Roessli D, Excoffier L. 2000. Arlequin: a software for population genetics data analysis. Version 2.000. Genetics and Biometry Lab, Department of Anthropology, University of Geneva, Switzerland.
- Schug MD, Hutter CM, Wetterstrand KA, Gaudette MS, Mackay TFC, Aquadro CF. 1998. The mutation rates of di-, tri- and tetranucleotide repeats in *Drosophila melanogaster*. *Mol Biol Evol.* 15:1751–1760.
- Schug MD, Mackay TFC, Aquadro CF. 1997. Low mutation rates of microsatellite loci in *Drosophila melanogaster*. *Nat Genet.* 15:99–102.
- Slatkin M, Hudson RR. 1991. Pairwise comparisons of mitochondrial DNA sequences in stable and exponentially growing populations. *Genetics.* 129:555–562.
- Strobeck C. 1987. Average number of nucleotide differences in a sample from a single subpopulation: a test for population subdivision. *Genetics.* 117:149–153.
- Tajima F. 1989. Statistical method for testing the neutral mutation hypothesis by DNA polymorphism. *Genetics.* 123:585–595.
- Tamura K. 1992. The rate and pattern of nucleotide substitution in *Drosophila* mitochondrial DNA. *Mol Biol Evol.* 9:814–825.
- Templeton AR, Crandall KA, Sing CF. 1992. A cladistic analysis of phenotypic associations with haplotypes inferred from restriction endonuclease mapping and DNA sequence data. III. Cladogram estimation. *Genetics.* 132:619–633.
- Turell MJ, Dohm DJ, Sardelis MR, O'Guinn ML, Andreadis TG, Blow JA. 2005. An update on the potential of North American mosquitoes (Diptera: Culicidae) to transmit West Nile virus. *J Med Entomol.* 42:57–62.
- Walton C, Handley JM, Tun-Lin W, Collins FH, Harbach RE, Baimai V, Butlin RK. 2000. Population structure and population history of *Anopheles dirus* mosquitoes in South-east Asia. *Mol Biol Evol.* 17:962–974.
- Weber JL, Wong C. 1993. Mutation of human short tandem repeats. *Hum Mol Genet.* 2:1123–1128.
- Weir B, Cockerham C. 1984. Estimating F-statistics for the analysis of population structure. *Evolution.* 38:1358–1370.
- Wright S. 1951. The genetical structure of populations. *Ann Eugen.* 15:323–354.
- Wright S. 1978. *Evolution and the genetics of populations. Volume 4. Variability within and among natural populations.* Chicago: University of Chicago Press.
- Zheng L, Wang S, Romans P, Zhao H, Luna C, Benedict MQ. 2003. Quantitative trait loci in *Anopheles gambiae* controlling the encapsulation response against *Plasmodium cynomolgi* Ceylon. *BMC Genetics.* 4:16.

Marcy Uyenyoyama, Associate Editor

Accepted February 26, 2007